Frontal Chromatography for Nonassociable and Micellar Systems

Noriaki FUNASAKI,* Sakae HADA, and Saburo NEYA
Kyoto Pharmaceutical University, Misasagi, Yamashina-ku, Kyoto 607
(Received August 9, 1993)

The continuous flow model of chromatography for computer simulations is developed and applied for nonassociable, dimerizing, and micellar systems. This model is more realistic than the discontinuous flow model, since the former takes into account the infinitesimal flow of the mobile phase. The frontal and zonal chromatograms of sucrose, a nonassociable solute, are determined on a Sephadex G-10 column as a function of the total sucrose concentration. The derivative of the frontal chromatogram at the leading boundary completely overlaps with that at the trailing boundary and has the same shape with the zonal chromatogram. Therefore the number of plate can be calculated from the observed derivative chromatogram. For some dimerizing systems the dimerization constant can be estimated from the concentration dependence of the derivative at the trailing boundary, if an appropriate correction is applied. Some characteristic parameters obtained from the derivative chromatogram of the micellar system provide information on the aggregation pattern. The observed results outlined above can be semiquantitatively predicted by the continuous flow model and by the discontinuous flow model, if the void volume and the number of plate are regarded as adjustable parameters in the latter model.

For the investigation of self-associating and micellar systems, a large amount of sample is often applied onto the column so that the plateau region can appear on the chromatogram. This method may be called frontal analysis.[1,2] On the other hand, in zonal analysis a small amount of sample is used, as is usually carried out. The zonal analysis has the advantage of requiring a small amount of sample over the frontal analysis and is well characterized for nonassociable systems. Micelle size and its dependence on concentration are estimated from the zonal analysis of some surfactants.[2] Comparison between the frontal and zonal analyses has been done for hexaethylene glycol dodecyl ether.[3] However, since the solute is diluted on the column during elution, quantitative information about self-associating behavior cannot be obtained from the zonal chromatogram.

The first derivative of the frontal chromatogram with respect to the elution volume can provide detailed information about self-association and must be also related with the resolution of the column, viz., the number of plate.[2] The number of plate is estimated from the peak on the zonal chromatogram.[4] This number may be expected to be obtained from the peak on the frontal derivative chromatogram, although this does not seem to have been tested against any experiment. Two plate theories are used for the zonal chromatogram; continuous flow model and discontinuous flow model.[4] The former model predicts the Poisson distribution for the chromatogram whereas the latter predicts the binomial distribution. The number of plate is calculated by applying the former model, since it is a more realistic model.[4] Computer simulations based on the latter model were applied for micellar systems,[5,6] but any computer program based on the former model has not yet been developed for micellar systems.

Characteristic values for the frontal chromatograms of micelle-forming systems were reported and compared with asymptotic theory and the discontinuous flow model.[6,7] More accurate experimental data are now available to test these theories and the continuous flow mode,[8—11] and realistic self-association models have recently been developed.[11] For instance, the shape of the derivative chromatogram for micellar systems has not fully been compared with theories, and the dimerization constants obtained from chromatographic centroid volumes and peak volumes are slightly different from ecah other.[12]

In this work we develop the continuous flow model for computer simulations, and apply it to the relationship between the frontal and zonal chromatograms of sucrose and comparison between simulation and experiment for dimerizing and micellar systems. Octaethylene glycol decyl ether ($C_{10}E_8$),[10] chlorpromazine hydrochloride (CPZ),[9] and 3-[(3-cholamidopropyl)dimethylammonio]-1-propanesulfonate (CHAPS)[8] are chosen as dimerizing and micellar systems, since these exhibit different aggregation patterns.

Theoretical

Frontal Chromatogram and Derivative. A schematic frontal chromatogram of a nonassociable solute and its first derivative with respect to the volume are shown in Fig. 1. The applied volume S of sample is large, so that the applied solution at concentration C_0 is eluted in the plateau region. We may assume that the equivalent sharp boundary for the leading or trailing edge of the solute zone on the frontal chromatogram is approximately the beginning (centroid) of the plateau region of the elution profile and satisfies the relationships:[1,2]

$$V_c' = \int_0^{C_0} V\mathrm{d}C/C_0 \quad \text{(leading boundary)} \tag{1}$$

and

$$V_c = \int_0^{C_0} V\mathrm{d}C/C_0 + S \quad \text{(trailing boundary)}. \tag{2}$$

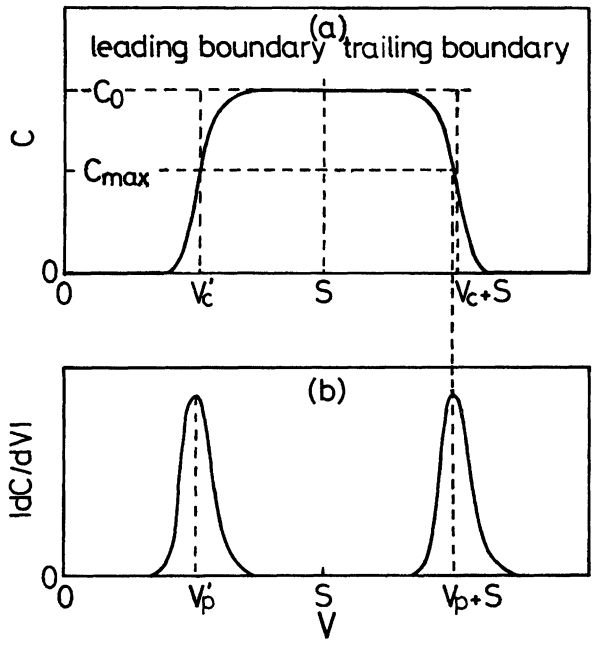

Fig. 1. Schematic frontal chromatogram (a) and its derivative (b).

For these determinations the volume coordinate V is assigned a zero value when the leading boundary of the applied sample enters the column bed. According to this approximation (called asymptotic theory), the elution curve for a nonassociable solute is expected to fall within a rectangle of height C_0 and width S. If all solute molecules applied are eluted out of the column, the two centroid volumes V_c' and V_c should be the same.

As a first approximation, the shape of the derivative chromatogram is expected to be the same with that of the zonal chromatogram. As is true for the zonal chromatogram, therefore, the peak height may be directly proportional to the applied concentration C_0 and the number N of plate may be evaluated from Fig. 2. The values of V_R and W are obtained from the triangle that is formed by the base line and two asymptotes to the derivative chromatogram: that is,[4]

$$N_{obsd} = 16(V_R/W)^2. \quad (3)$$

These two presumptions will be tested against both experiment and theory below.

Plate Theory. In plate theory, it is assumed that the column bed consists of successive plates of number N. Two models based on the plate theory are shown in Fig. 3.[4] The total volume of the mobile phase is V_0 and the concentration of solute in the mobile phase of the i-th plate is C_i. Since the discontinuous flow model has already been reported in detail,[5,6] a brief explanation will be given herein. When eluent of the volume V_0/N is added, as shown in Fig. 3a, the concentration in the i-th mobile phase is changed from C_i to C_{i-1}. When equilibration of partition of the solute between the mobile and stationary phases has been established,

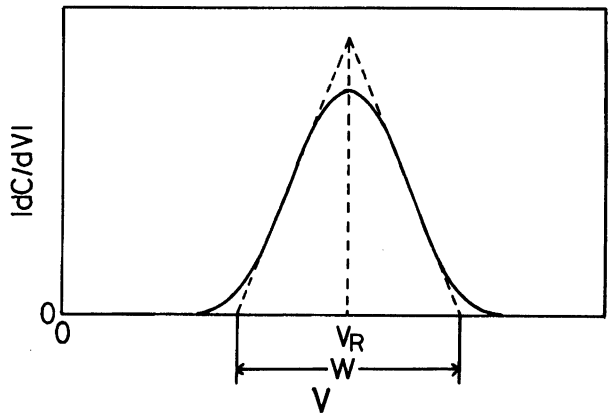

Fig. 2. Definition of a triangle for the calculation of the number of plate from the derivative chromatogram.

the new concentration in the i-th mobile phase becomes C_i'. When this process is repeated, we can obtain a chromatogram; that is, the relationship between C_N' and V. In the continuous flow model, eluent of the volume V_0/ND is added. Then the mobile phase in each plate is homogenized and the concentration in the i-th mobile phase is changed to $[C_i(D-1)+C_{i-1}]/D$. After partition equilibration between the mobile and stationary phases, the new concentration in the i-th mobile phase becomes C_i'. When this process is repeated, we can obtain a chromatogram. When D is large, the flow of eluent becomes practically continuous. Therefore, this is termed continuous flow model.[4]

The discontinuous flow model may be valid for counter current distribution. Since the continuous flow model is more realistic than the discontinuous model, Eq. 3 is derived from the former model.[4] For both the models, the gel–water partition coefficient of a solute having the centroid volume V_c can be written as $(V_c-V_0)/V_0$,[4] and self-association in the mobile phase is assumed to be rapid.

Experimental

Materials. Sucrose was purchased from Tokyo Kasei Organic Chemicals. CPZ (Sigma), $C_{10}E_8$ (Nikko Chemicals), and CHAPS (Dojindo) were the same with those already reported.[8—10] Sephadex G-10 (Pharmacia) was treated according to the suggestions of the manufacturer. The ion-exchanged water was twice distilled and degassed before use.

Methods. In GFC experiments of sucrose, a column of a total gel volume of $V_t=22.70$ cm^3 was jacketed to maintain it at a constant temperature of 298 K. The void volume V_0 was determined to be 7.49 cm^3 with Blue Dextran (Pharmacia). The rate of flow was monitored and was about 0.4 cm^3 min^{-1}. The elution process was monitored continuously with a refractive index detector and recorded with a data processor. The observed refractive index data were converted to total solute concentrations. The position and height of the peak in the derivative chromatogram were determined by a polynomial approximation. All GFC experi-

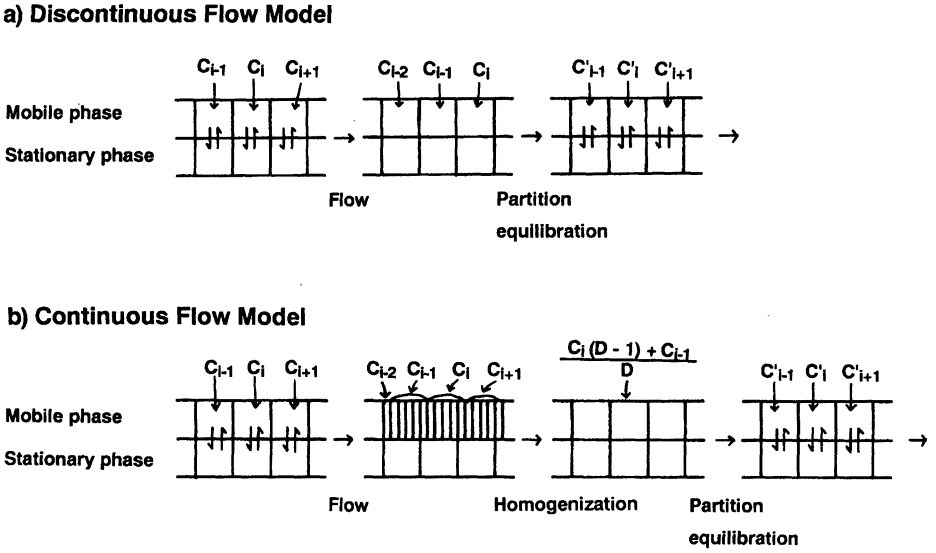

Fig. 3. Explanation of two flow models for the chromatogram.

ments of CPZ,[9] $C_{10}E_8$,[10] and CHAPS[8] were carried out on Sephadex G-10 columns at 298 K. As eluent, water was used for $C_{10}E_8$ and CHAPS and 0.15 mol dm^{-3} sodium chloride solution was for CPZ. All computer simulations were carried out with a personal computer, and details of the simulation procedure were reported elsewhere.[6]

Results and Discussion

Nonassociable System. The frontal derivative chromatograms at four applied concentrations of sucrose are shown in Fig. 4. The centroid volume, the peak volume, and the peak height are evaluated at the leading and trailing boundaries and are shown in Table 1. These centroid and peak volumes are independent of the applied concentration and are close to each other. The latter result means that the peak is almost symmetric. The peak height is directly proportional to the applied concentration of sucrose. This is an important result. When the trailing boundary volume is plotted against V minus S, the derivative chromatograms at both boundaries are practically overlapped. As Table 1 shows, therefore, the number N_{obsd} of plate calculated from Eq. 3 using the frontal derivative chromatogram is the same at both boundaries, regardless of the applied concentration.

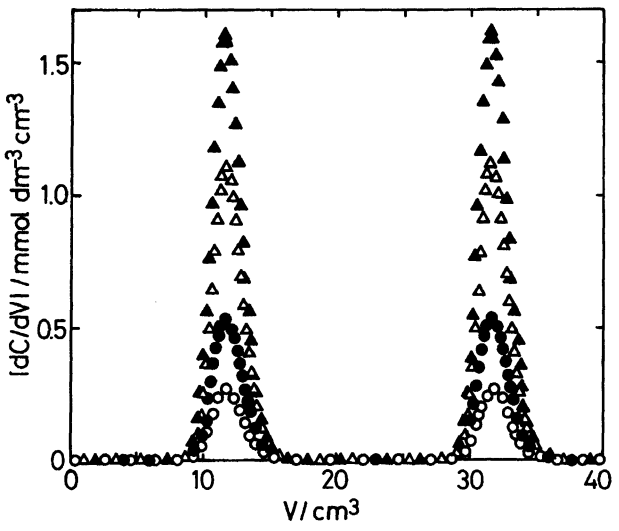

Fig. 4. Concentration dependence of the derivative chromatograms of sucrose in water at four applied concentrations (mmol cm^{-3}): ○, 0.7654; ●, 1.5133; △, 3.0791; ▲, 4.4347.

Under the same conditions, the zonal chromatograms of sucrose at four applied concentrations are determined, where the applied volume of sample is kept constant at 0.10 cm^3. As Table 2 shows, both the peak volume V_p and the number N_{obsd} of plate are almost independent of the applied concentration and are close to those obtained from the frontal chromatogram (Table 1). The peak height C_{max} is almost proportional to the applied concentration. Thus, the shape of the zonal chromatogram is identical to that of the frontal derivative chromatogram.

On the basis of the continuous flow model, the frontal chromatogram was simulated by employing the values of C_0=1 mmol dm^{-3}, V_0=100 cm^3, V=230 cm^3, N=100, and D=1 to 100. The derivative chromatogram at the leading boundary is identical with that at the trailing boundary. In Fig. 5, N_{obsd} denotes the N value calculated from Eq. 3 using the simulated derivative chromatogram. This value is much larger than the input N value (100), when D is smaller than 10. The ratio of N_{obsd}/N at D=1 corresponds to the discontinuous flow model. Thus, the result of Fig. 5 demonstrates that the continuous flow model is more realistic than the discontinuous flow model and that the D value employed should be larger than 10. A value of D=10 is employed for all calculations hereafter. The continuous flow model with the input values of N=105, V_0=7.49

Table 1. Observed Frontal Chromatographic Data on Sucrose in Water at 298 K

C	Leading boundary				Trailing boundary			
mmol dm^{-3}	V_c'/cm^3	V_p'/cm^3	dC/dV/mmol dm^{-3} cm^{-3}	N_{obsd}	V_c/cm^3	V_p/cm^3	dC/dV/mmol dm^{-3} cm^{-3}	N_{obsd}
0.7654	11.71	11.78	0.268	106	11.78	11.78	0.266	106
1.5133	11.72	11.79	0.536	100	11.78	11.79	0.540	100
3.0791	11.83	11.72	1.116	106	11.82	11.73	1.124	106
4.4347	11.83	11.73	1.612	108	11.79	11.73	1.623	108
Average	11.77	11.76	—	105	11.79	11.76	—	105

Table 2. Observed Zonal Chromatographic Data on Sucrose in Water at 298 K

C/mol dm^{-3}	V_p/cm^3	C_{max}/mol dm^{-3}	N_{obsd}
0.03758	11.81	0.00136	106
0.05953	11.69	0.00212	106
0.08478	11.75	0.00307	108
0.11569	11.69	0.00412	106
Average	11.74	—	107

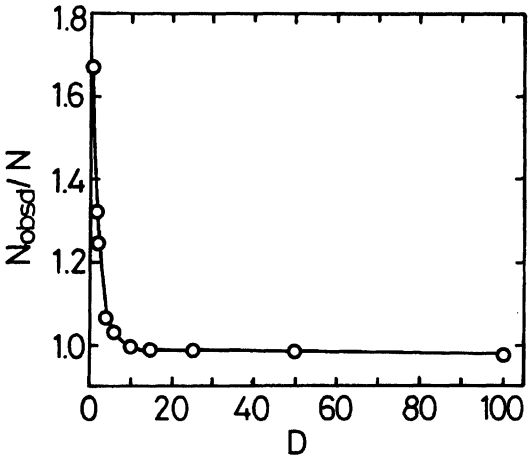

Fig. 5. Ratio of the observed number of plate to the input N value as a function of the input number D of subdivision of a plate. The N value is kept constant at 100, whereas the D value is changed.

cm^3, $D=10$, and $V=11.80$ cm^3 well reproduces the observed results shown in Tables 1 and 2 and in Fig. 4.

Close chromatograms are obtained by the discontinuous flow model with two sets of input parameters, $N=105$, $V_0=1.0$ cm^3, and $V=11.80$ cm^3 and $N=40$, $V_0=7.5$ cm^3, and $V=11.80$ cm^3, but the void volume or the number of plate is much smaller than the observed value. That is, the void volume and the number of plate must be regarded as adjustable parameters in the discontinuous flow model.

Dimerizing Systems. In general, the derivative chromatograms of polymerizing systems at the trailing boundary are bimodal, whereas that of the dimerizing system is unimodal.[1,6] For the dimerizing system, the peak of the derivative chromatogram at the trailing boundary is smaller than that at the leading boundary. By this feature, the dimerizing system can be distinguished from the nonassociable system.[6] According to asymptotic theory, the peak position V_p at the trailing boundary for the dimerizing system is related with the concentration C_{max} (Fig. 1) at V_p as follows:[1,13]

$$[(V_1 - V_2)/(V_p - V_2)]^2 = 1 + 8k_{2p}C_{max}. \quad (4)$$

Here V_2 denotes the centroid volume of the dimer. When the Sephadex G-10 gel is used, this value may be evaluated by extrapolation of V_c to infinite concentration. If Eq. 4 is valid, we may evaluate the dimerization constant (k_{2p}) from the concentration dependence of the trailing peak position V_p. For CPZ we have already reported the observed values of V_p, C_{max}, V_1, and V_2 in 0.15 mol dm^{-3} sodium chloride solution as a function of the total CPZ concentration.[9,12] The values of V_1 and V_2 are shown in Table 3. Using these values, we plotted the values of $[(V_1-V_2)/(V_p-V_2)]^2$ against C_{max}, but the relation between these values is nonlinear and the

Table 3. Observed and Estimated Values from Chromatographic Data for Micellar Systems

	CHAPS[a]	CPZ[b]	$C_{10}E_8$[c]
	Observed value		
N_{obsd}	16	31	40
V_t/cm^3	17.70	7.78	22.46
V_0/cm^3	6.36	2.56	7.89
V_1/cm^3	14.81	112.64	16.47
V_2/cm^3	6.36	2.56	7.89
V_m/cm^3	6.36	2.56	7.89
V_{1p}^0/cm^3	13.87	111.50	15.71
V_{2p}^∞/cm^3	5.62	2.57	7.63
	Discontinuous flow model		
N	14	30	40
V_0/cm^3	4.0	1.0	5.0
V_{1p}^0/cm^3	14.33	109.0	16.19
V_{2p}^∞/cm^3	6.38	2.56	7.78
	Continuous flow model		
N	16	31	40
D	10	10	10
V_0/cm^3	6.36	2.56	7.89
V_{1p}^0/cm^3	13.92	111.0	16.08
V_{2p}^∞/cm^3	6.03	2.56	7.63

a) Observed values taken from Refs. 8 and 12. b) Observed values taken from Refs. 9 and 12. The reason why the values of V_1 and V_{1p}^0 are much larger than the total bed volume V_t is attributable to aromatic adsorption (N. Funasaki, S. Hada, and S. Neya, *J. Colloid Interface Sci.*, **156**, 518 (1993)). c) Observed values taken from Refs. 10 and 12.

intercept of the ordinate is not unity (data not shown). This failure of Eq. 4 is ascribed to the assumption of the asymptotic theory that the centroid volume V_c is identical to the peak position V_p. The same conclusion is reached for CHAPS[8] (data not shown).

Therefore we modified Eq. 4 as follows:

$$[(V_{1p}^0 - V_{2p}^\infty)/(V_p - V_{2p}^\infty)]^2 = 1 + 8k_{2p}C_{max}. \quad (5)$$

This equation may hold true also for systems including the dimer and higher multimers at so low concentrations that the multimers are negligible.[12] The value of V_{1p}^0 can be estimated by extrapolation of V_p to infinite dilution. For the Sephadex G-10 gel whose pores are smaller than dimers, the value of V_{2p}^∞ may be obtained by extrapolation of the micellar peak volume V_{mp} or V_p' to $1/C_0=0$ or it may be taken as the peak volume of a large molecule, such as Blue Dextran. Figure 6a shows the plot according to Eq. 5 for CPZ. The value of V_{1p}^0 was estimated to be 111.5 cm^3 by extrapolation of the observed V_p values to infinite dilution and a value of $V_{2p}^\infty=2.57$ cm^3 is used as the observed V_p value for Blue Dextran. The dimerization constant k_{2p} evaluated from the linear portion in Fig. 6a is shown at the column k_{2p} in Table 4. The k_2 value (k_{2c}) estimated from the observed V_c data is 0.124 dm^3 mmol^{-1} and is very close to the k_2 value obtained from spectrophotometric measurements.[9] Thus, the k_{2c} value is reliable.[12] The deviation from the linearity of Eq. 5 at large C_{max} values (viz., at high CPZ concentrations) will be attributable to neglect of oligomers, such as trimers, tetramers, and so on.

The solid line in Fig. 6a is obtained on the basis of the continuous flow model. The aggregation model that CPZ forms the dimer and the 38-mer with aggregation constants of $k_2=0.124$ dm^3 mmol^{-1} and $K_{38}=9.39\times10^{-22}$ dm^{111} mmol^{-37} (model I of Ref. 9) is used for the simulation of the chromatogram. The K_{38} value is the equilibrium constant for the formation of 38-mer from 38 monomers. The void volume is set as the observed V_c value for Blue Dextran. The number of plate is estimated from the trailing derivative chromatogram at a very low concentration by using Eq. 3. The centroid volumes, V_1 and V_m, of the monomer and the aggregates are estimated by extrapolation of the observed V_c values to infinite dilution and concentration.[9] These values of k_2, K_{38}, N, V_0, and V_m, $D=10$, and an applied concentration are used as the input data to calculate a frontal chromatogram of CPZ. The V_p values are obtained from these calculated chromatograms and are used to extrapolate a value of $V_{1p}^0=111.0$ cm^3 to infinite dilution and the V_{mp} values calculated are used to estimate a value of $V_{2p}^\infty=2.56$ cm^3 by extrapolation to infinite concentration. As Table 3 shows, the estimated values of V_{1p}^0 and V_{2p}^∞ are slightly different from those obtained experimentally. As Fig. 6a shows, the agreement between theory and experiment is very good at low concentrations. The dimerization constant obtained from the linear portion in Fig. 6a is shown at column k_{2p} in Table 4. If CPZ forms the dimer only with a dimerization constant of $k_2=0.124$ dm^3 mmol^{-1}, the linear relationship observed at low concentrations in Fig. 6a also holds at higher concentrations (data not shown).

The dashed line in Fig. 6a is calculated on the basis of the discontinuous flow model with the input values of $N=30$ and $V_0=1.0$ cm^3 and k_2, K_{38}, V_1, and V_m used for the solid line. At a number of concentrations, chromatograms are calculated. From these chromatograms the V_p values are obtained and are used to estimate the values of V_{1p}^0 and V_{2p}^∞ shown in Table 3. The difference between the continuous and discontinuous flow models is small, as shown in Fig. 6a, since the number of plate and the void volume are regarded as adjustable parameters in the latter model.

Figure 6b shows the observed peak volume data on CHAPS, taken from Ref. 12. The treatment of chromatographic data is the same with that of CPZ. The solid line is calculated on the basis of the continuous flow model using a stepwise aggregation model (model M9 of Ref. 8) which accounts for all aggregate species of CHAPS. The dashed line is calculated on the basis of the discontinuous flow model with the input values of $N=14$ and $V_0=4.0$ cm^3 using the same aggregation model (model M9). As Table 4 shows, the k_{2p} value is larger than the k_{2c} value obtained from the observed centroid volume data. At high concentrations of CHAPS the relation deviates positively from the linearity exhibiting dimerization at low concentrations, in contrast with CPZ (Fig. 6a). These results are explicable theoretically, as shown by either the solid line or the dashed line.

The dimerization constant of $C_{10}E_8$ is determined from each of the observed V_c and V_p data, as shown in Table 4. The observed V_p values and their analysis based on Eq. 5 have been reported.[12] For the simulation of the chromatogram, we need any aggregation model of $C_{10}E_8$. The standard free energy of i-mer formation of $C_{10}E_8$ may be expressed as

Table 4. Observed and Calculated Values of the Cmc and Dimerization Constant

	CHAPS[a]	CPZ[b]	$C_{10}E_8$[c]	Average
Observed value				
cmc/mmol dm^{-3}	5.5	5.4	1.03	—
k_{2c}/mol^{-1} dm^3	4.6	124	7.7	—
k_{2p}/mol^{-1} dm^3	5.6	142	8.7	—
k_{2p}/k_{2c}	1.22	1.15	1.13	1.17
Calculated from discontinuous flow model				
k_{2p}/k_2	1.35	1.24	1.25	1.28
Calculated from continuous flow model				
k_{2p}/k_2	1.22	1.23	1.22	1.22

a) Observed values taken from Refs. 8 and 12. b) Observed values taken from Refs. 9 and 12. c) Observed values taken from Refs. 10 and 12.

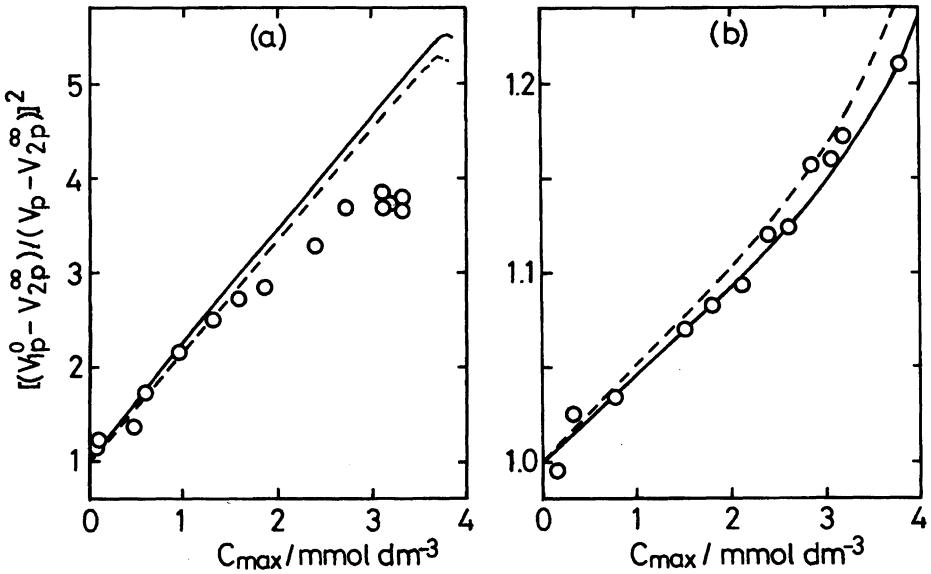

Fig. 6. Plot of the peak data according to Eq. 5 for CPZ (a) and CHAPS (b). The solid and dashed lines are calculated on the basis of the continuous and discontinuous flow models, respectively. The input values of N, D, V_0, V_1, and V_m for chromatographic simulations are shown in Table 3.

$$i\Delta G_i^\circ/kT = -11.29(i-1) + 23.71(i^{2/3}-1) + 1.475(i^{4/3}-1). \quad (6)$$

This equation is based on the Tanford micellization model for spherical micelles and is employed for simplicity of calculation.[10] The molarity C_i (mmol dm^{-3}) of i-mer of $C_{10}E_8$ can be calculated from

$$C_i = C_1^i \exp(-i\Delta G_i^\circ/kT). \quad (7)$$

The total concentration C can be calculated from the monomer concentration C_1:

$$C = \sum_{i=1}^{\infty} iC_1^i \exp(-i\Delta G_i^\circ/kT). \quad (8)$$

From Eq. 8 we can calculate the micellar concentration, $C - C_1$, and use it to calculate the micellar concentration in the gel phase.[10] Further details of experiments and computer simulations on $C_{10}E_8$ have been reported.[10,11] Other aggregation models for $C_{10}E_8$ are available[11] and give similar results (data not shown).

The theoretical k_{2p} values are also determined on the basis of the continuous flow model and the discontinuous flow model using Eq. 8. In the latter model, the input data are $V_0 = 5.0$ cm^3, $N = 30$, $V_1 = 16.47$ cm^3, and $V_m = 7.89$ cm^3. Similarly to CPZ, the plot based on Eq. 5 deviates negatively from the linearity at high concentrations (data not shown). For compounds exhibiting highly cooperative micellization, such as $C_{10}E_8$ and CPZ, the trailing derivative chromatogram split into two clear peaks above the critical micelle concentration (cmc) and the plot of Eq. 5 deviates negatively from the linearity at high concentrations. For a compound, such as CHAPS, the trailing derivative chromatogram does not show two clear peaks (Fig. 7)[8] and the plot of Eq. 5 deviates positively at high concentrations.

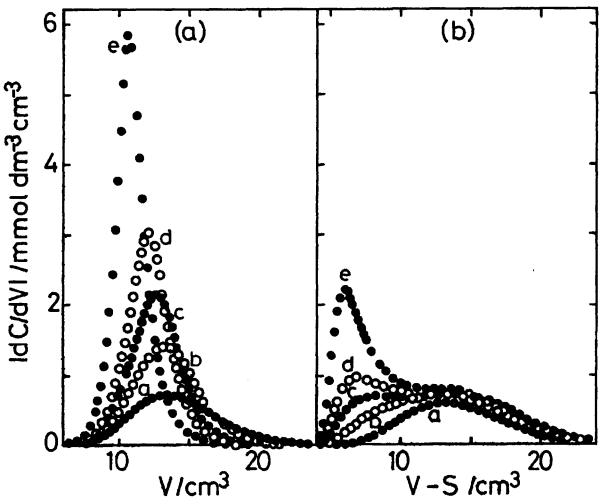

Fig. 7. Observed leading (a) and trailing (b) chromatograms of CHAPS on a Sephadex G-10 column at five CHAPS concentrations (mmol dm^{-3}): a, 5.3555; b, 8.0962; c, 9.6878; d, 11.1872; e, 15.452.

As Table 4 shows, the values of k_{2p}/k_{2c} and k_{2p}/k_2 are about 1.2, regardless of the compounds, theories, and experiments. Thus, Eq. 5 is also an approximation and may be modified as

$$[(V_{1p}^0 - V_{2p}^\infty)/(V_p - V_{2p}^\infty)]^2 = 1 + 9.6k_{2p}C_{max}. \quad (9)$$

Micellar Systems. At very low concentrations, CPZ, CHAPS, and $C_{10}E_8$ form mainly dimers. Above the cmc (Table 4), the micellar aggregation numbers of CPZ[9] and $C_{10}E_8$[10] are about 38 and 46, respectively and that of CHAPS increases gradually with increasing concentration;[8] e. g., the weight average aggregation number of CHAPS is 15 at 30 mmol dm^{-3}. Several

characteristic quantities for the frontal chromatograms of these systems will be considered below.

Frontal chromatograms of CHAPS in water on a Sephadex G-10 column were obtained at 25 CHAPS concentrations and 298 K, although no leading chromatogram at high concentrations was reported.[8] Observed derivative chromatograms at five CHAPS concentrations are shown in Fig. 7. Their simulations based on the continuous flow model are shown in Fig. 8. Those based on the discontinuous flow model at the trailing boundary were reported.[8] The procedure and conditions for these simulations are the same with the dimerizing system described above.

Figure 9 shows the peak height data on CHAPS as a function of CHAPS concentration. Below 2 mmol dm^{-3}, the height of the trailing peak is very close to that of the leading peak and is directly proportional to the concentration. As these results demonstrate, the peak height at neither the leading boundary nor the trailing is proportional to the applied concentration of CHAPS at concentrations higher than 2 mmol dm^{-3}, being different from the nonassociable system (Table 1). The reason for these results is that almost no CHAPS molecule self-associates at concentrations lower than 2 mmol dm^{-3}. At concentrations higher than 2 mmol dm^{-3}, the height of the trailing peak is smaller than that of the leading peak. Around 10 mmol dm^{-3}, the trailing peak is bimodal and above such a concentration, the monomer peak becomes a shoulder of the micellar peak. From the observed derivative chromatograms, therefore, accurate monomer peak heights at CHAPS concentrations higher than 11 mmol dm^{-3}, cannot be determined. At CHAPS concentrations lower than 9 mmol dm^{-3}, the micelle peak becomes a shoulder of the monomer peak and therefore no accurate peak height can be determined from the observed derivative chromatograms (Fig. 7).[8]

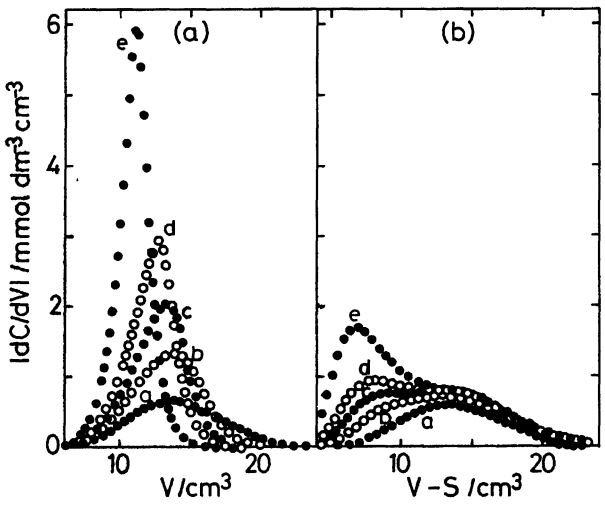

Fig. 8. Simulated chromatograms of CHAPS based on the continuous flow model, corresponding to Fig. 7. The input values of N, D, V_0, V_1, and V_m for chromatographic simulations are shown in Table 3.

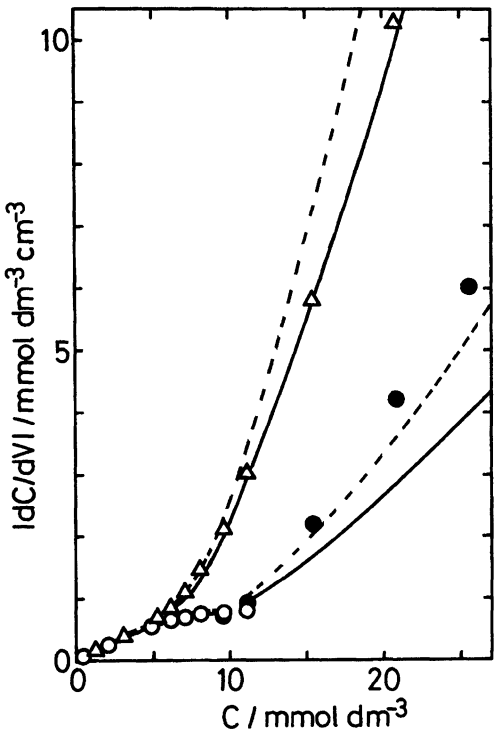

Fig. 9. Peak heights at the leading boundary (△) and for the monomer (○) and the micelle (●) at the trailing boundary on the derivative chromatogram of CHAPS. The solid and dashed lines are calculated on the basis of the continuous and discontinuous flow models, respectively. The input values of N, D, V_0, V_1, and V_m for chromatographic simulations are shown in Table 3.

The solid lines in Fig. 9 are calculated by the continuous flow model with the input values of $N=16$ and $V_0=6.36$ cm^3. This model very well predicts the heights of the leading peak and the monomer peak at the trailing boundary, but does not well do so the height of the miceller peak at the trailing boundary. The dashed lines are calculated on the basis of the discontinuous flow model with $N=14$ and $V_0=4.0$ cm^3, which are regarded as adjustable parameters. This model reasonably reproduces the heights of both the leading peak and the trailing micellar peak.

Figure 10a shows the observed derivative chromatograms of $C_{10}E_8$ at three concentrations and $S=$ 20.00 cm^3. Around the cmc (1.03 mmol dm^{-3}) the changes in shape of the chromatogram with increasing concentration are more abrupt than those for CHAPS shown in Fig. 9. For the leading boundary the relationship between the peak height and the total concentration consists of two almost straight lines with the intersection at the cmc. For the trailing boundary, the monomer peak height is almost proportional to the total concentration below the cmc and remains almost unchanged with increasing concentration above the cmc. The micellar peak height at the trailing boundary is al-

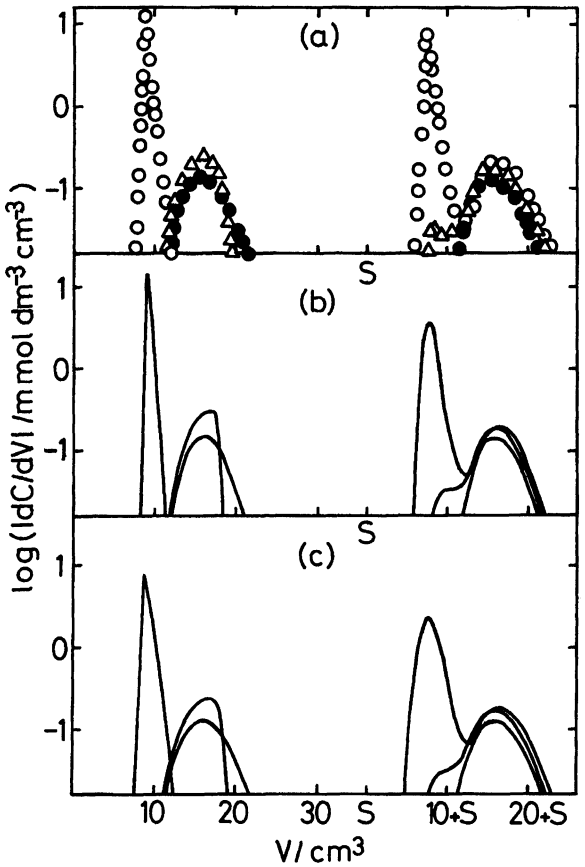

Fig. 10. Observed derivative chromatogram (a) of $C_{10}E_8$ and the corresponding chromatogram calculated from the discontinuous flow model (b) and from the continuous flow model (c) at three $C_{10}E_8$ concentrations (mmol dm^{-3}): ●, 0.8263; △, 1.2140; ○, 8.0352. The input values of N,D, V_0,V_1, and V_m for chromatographic simulations are shown in Table 3.

most proportional to the micellar concentration, viz., $C-$cmc (data not shown). Figures 10b and 10c show the corresponding simulations based on the discontinuous and continuous flow models, respectively.

For $C_{10}E_8$ and CPZ, the derivative chromatogram at the trailing boundary above the cmc has a clear minimum, e. g., as shown for $C_{10}E_8$ in Fig. 10. In Fig. 11 the concentration C_{min} at the minimum is shown as a function of the total concentration. The C_{min} value for $C_{10}E_8$ appears to be almost independent of the porosity of the gel used,[7,10] although the accuracy in C_{min} is now much improved by advances in our experimental skill and instrumentation. This value for $C_{10}E_8$ only slightly increases or remains unchanged with increasing concentration. The C_{min} value for CPZ decreases with increasing concentration above the cmc. In general, when oligomerization constants are large, the C_{min} value appears to decrease with increasing concentration. The theoretical C_{min} values calculated from the discontinuous and continuous flow models are very close to each other, as shown by the solid lines in Fig. 11, and

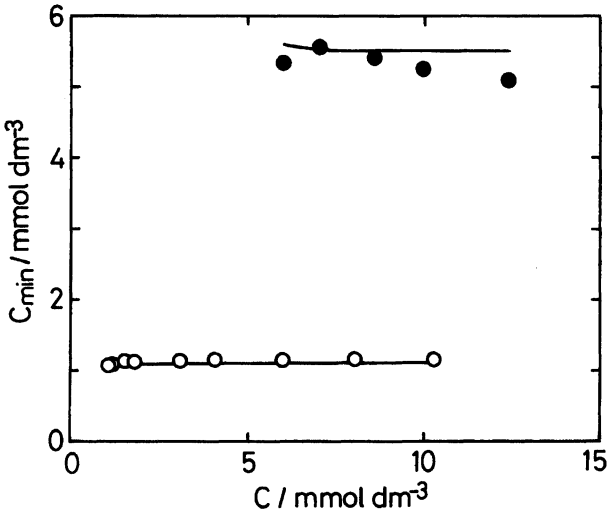

Fig. 11. Concentration dependence of C_{min} for $C_{10}E_8$ (○) and CPZ (●). The solid lines are theoretically calculated; the continuous and discontinuous flow models predict very close results. The input values of N,D, V_0,V_1, and V_m for chromatographic simulations are shown in Table 3.

only slightly decrease or remain constant with increasing concentration for both $C_{10}E_8$ and CPZ. The C_{min} value is slightly larger than the monomer concentration and is almost equal to the cmc (Fig. 11 and Table 4).

Conclusions

For sucrose, a nonassociable solute, the derivative chromatograms at the leading and trailing boundaries overlap completely and have the same shape with the zonal chromatogram. The peak height on the derivative chromatogram is directly proportional to the concentration applied. The peak volume on the derivative chromatogram is identical with that on the zonal chromatogram. Thus, the number of plate can be estimated from the frontal derivative chromatogram using Eq. 3.

The continuous flow model is more realistic than the discontinuous flow model often used, since the former takes into account the infinitesimal flow of the mobile phase. The number of subdivision of a plate in the continuous flow model may be set equal to 10. The observed chromatograms for sucrose are well-predictable by the continuous flow model using the observed values of the void volume and the number of plate. This is the advantage over the discontinuous model, although the former model has the disadvantage of requiring more computing time than the latter.

For self-associating systems, the dimerization constant can be estimated from the concentration dependence of the trailing peak volume using Eq. 9. This equation is a modification of Eq. 4. The peak volumes, V_{1p}^0 and V_{2p}^∞, for the monomer and the dimer should be used instead of the centroid volumes V_1 and V_2. A correction factor, which is estimated from experimental results and the continuous and discontinuous flow

models independently, should be introduced in Eq. 5.

Some characteristic parameters on the derivative chromatograms of micellar systems depend strongly on the pattern of micellization. For $C_{10}E_8$ exhibiting a high cooperativity in micellization, the relationship between the peak height and the total concentration consists of two almost straight lines with a sharp break at the cmc and the C_{min} value only slightly increases with increasing concentration. For CHAPS exhibiting a low cooperativity, the peak height increases nonlinearly with increasing concentration. For CPZ having a large dimerization constant, the C_{min} value slightly decreases with increasing concentration. These features for the micellar systems can be reproduced by the continuous flow model and by the discontinuous flow model in which the void volume and the number of plate are regarded as adjustable parameters.

Thus, the physical meaning of the frontal chromatogram and its derivative for nonassociable and self-associating systems is established on the basis of theory and experiment. The above results are particularly useful to the elucidation of the aggregation behavior of complicated systems, such as micellar systems.

Thanks are due to Miss Noriko Nakazawa and Messrs. Kaoru Nishi and Chuhei Majima for some experiments and computations.

References

1) G. K. Ackers, *Adv. Protein Chem.*, **24**, 343 (1970).
2) N. Funasaki, *Adv. Colloid Interface Sci.*, **43**, 87 (1993).
3) N. Funasaki, S. Hada, and S. Neya, *J. Phys. Chem.*, **92**, 3488 (1988).
4) A. I. M. Keulemans, "Gas Chromatography," Reinhold, New York (1959), Chap. 4.
5) T. Nakagawa and H. Jizomoto, *Kolloid-Z. Z. Polym.*, **234**, 1124 (1970).
6) N. Funasaki, S. Hada, and S. Neya, *Bull. Chem. Soc. Jpn.*, **62**, 380 (1989).
7) N. Funasaki, S. Hada, and S. Neya, *J. Phys. Chem.*, **92**, 7112 (1988).
8) N. Funasaki, S. Hada, and S. Neya, *J. Phys. Chem.*, **95**, 1846 (1991).
9) N. Funasaki, S. Hada, and J. Paiement, *J. Phys. Chem.*, **95**, 4131 (1991).
10) N. Funasaki, H.-S. Shim, and S. Hada, *J. Chem. Soc., Faraday Trans.*, **87**, 957 (1991).
11) N. Funasaki, H.-S. Shim, and S. Hada, *J. Phys. Chem.*, **96**, 1998 (1992).
12) S. Hada, S. Neya, and N. Funasaki, *Bull. Chem. Soc. Jpn.*, **65**, 314 (1992).
13) G. K. Ackers and T. E. Thompson, *Proc. Natl. Acad. Sci. U. S. A.*, **53**, 341 (1965).